ISBN: 978-3-95450-132-8 doi:10.18429/JACoW-IPAC2014-MOPRI043

STUDY OF A C-BAND STANDING-WAVE GUN FOR THE SwissFEL INJECTOR

M. Schaer, S. Bettoni, A. Citterio, P. Craievich, M. Negrazus, L. Stingelin, R. Zennaro
Paul Scherrer Institut, Switzerland

Abstract

The baseline design of the SwissFEL injector foresees the "PSI Gun 1", a 2.6-cell RF photo-cathode gun operating at S-band frequency, as the electron source. In this paper a new design is presented where a 5.6-cell C-band gun could replace the PSI Gun 1 with no impact on the rest of the injector setup. A conservative maximum gradient of 135 MV/m at the cathode is assumed which drives the electron beam faster into the relativistic regime and therefore allows to tolerate larger charge densities. The presented solution also foresees a coaxial RF coupling from the cathode side in order to place the gun solenoid as near to the photo-cathode as possible, improving the emittance compensation. Astra simulations showed that the transverse beam brightness can be doubled before the first bunch compressor preserving the low transverse emittance value as compared to the current design for the S-band injector configuration of SwissFEL.

INTRODUCTION

The SwissFEL injector test facility has been running with the "CTF2 Gun 5" photo-cathode RF gun [1] since August 2010, showing very promising beam parameters [2] in view of the final SwissFEL user facility [3] whose first beam is planned for the end of 2016. This gun has very recently been replaced by the S-band "PSI Gun 1" [4], which is the baseline for the first operation of the SwissFEL injector. Experimental results concerning beam quality are expected soon and will be compared with the promising predictions from simulations [5].

Preliminary simulations of the SwissFEL injector with a 3.6-cell C-band photo-cathode RF gun have shown that there is still potential for important improvements in the RF design [6]. In particular, it was shown that there is the possibility to halve the bunch length while preserving the low slice emittance, which corresponds to twice the transverse brightness. Doubling the peak current would relax the compression factor to be achieved in the two bunch compressors reducing the risk of deluting the beam quality (transverse emittance and energy spread).

The need for space for beam diagnostics after the gun is satisfied by adding two additional cells which boost the energy up to ~ 10 MeV at the exit of the gun and shift the invariant-envelope matching point, i.e. the entrance of the first traveling-wave structure, to ~ 2 m from the cathode.

In this paper the improved beam dynamics results are finalized into an RF and magnet design which fulfill all requirements and constraints of the SwissFEL injector.

RF DESIGN

The choice of increasing the frequency and designing a gun operating at C-band is especially motivated by the shorter filling-time and the experimental evidence indicating that this enables higher accelerating gradients [7]. The established C-band technology for the SwissFEL main linac provides the necessary confidence to succesfully operate a cavity at this frequency. Moreover, in the specific case of the SwissFEL injector, a frequency mismatch between gun and booster (S-band) potentially reduces the dark current transported up to the first bunch compressor by a factor of 21 [6].

Doubling the frequency of the cavity roughly coincides with halving the mechanical dimensions of its cells. In terms of mechanical limitations, but not only, an RF coaxial coupling from the cathode side, like that presented in Fig. 1, has several advantages. First, no longitudinal constraint is

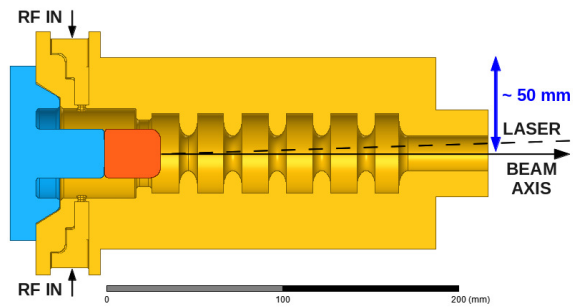

Figure 1: 2D overview of the gun RF design. Gun main body (yellow), removable back plate (blue) and removable cathode (orange). Near to the back plate, the two tapered input wave guides are clearly visible. The material of the components is copper.

introduced like in the case of a wave guide coupling to one of the full cells, where the solenoid is typically shifted away from the cathode. This problem could be solved with a coaxial coupling at the exit of the gun like in [8], but such a solution would further reduce the available space for the laser coupling to less than the iris aperture. In addition, the gun design is further simplified since it does not require racetrack geometry for compensation of quadrupolar components which are usually introduced by the geometrical asymmetries of the coupling cells.

In the coaxial region it was possible to design some gaps with vanishing electric and magnetic fields (see Fig. 2), so that it is possible to assemble the gun with three mechanical independent pieces without the need of special RF contacts because of the absence of current flows. As it can be seen

ISBN: 978-3-95450-132-8 doi:10.18429/JACoW-IPAC2014-MOPRI043

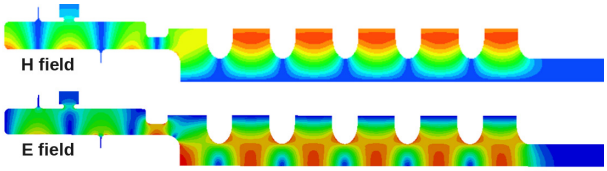

Figure 2: 2D distribution of the complex magnitude of magnetic and electric field computed by the frequency domain solver.

from Fig. 1, the back plate can be easily retracted for cathode exchange and reconnected to the gun main body.

The HFSS simulation of Fig. 2 shows that the chosen iris geometry keeps the surface electric fields below the maximum electric field on-axis (equal to that at the cathode). The maximum magnetic field is at the coupler iris and it is small enough to keep the temperature rise due to pulse heating below 50 K. The longitudinal electric field on-axis computed by the eigenmode solver is well balanced (see Fig. 3, green curve). The estimated quadrupole contribution was evaluated by computing the integrated beam voltage V_z at $r = 6$ mm for different azimuthal angles $\phi \in [0, \pi/2]$. The relative difference between maximum ($\phi = 0$) and minimum ($\phi = \pi/2$) was found to be $|\Delta V_z|_{r=6\,\mathrm{mm}}/|V_z|_{r=0} < 10^{-4}$.

The main RF cavity parameters are listed in Tab. 1. Assuming a realistic input power of 32.0 MW, a square pulse of 387 ns is required to reach 135 MV/m at the cathode. To reach the same field in steady state (defined as $t \geq 3\tau_L = 657$ ns) an input power less than 24.4 MW is required. Fig. 3 shows the complex electric field of the adjacent mode computed at the working frequency $f_0 = 5.712$ GHz and the field of the operating mode.

The effect of the adjacent mode in the transient regime is currently under study. Calculations also showed the possibility to increase the iris aperture to $i = 12$ mm in order to gain

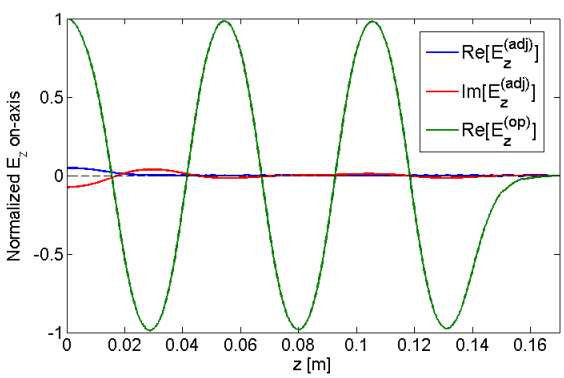

Figure 3: Real and imaginary components of the longitudinal electric field E_z on-axis from the frequency domain solver. The real part $\mathrm{Re}[E_z] = \mathrm{Re}[E_z^{(op)}] + \mathrm{Re}[E_z^{(adj)}]$ was split into operating (op) and adjacent (adj) mode contribution. $\mathrm{Re}[E_z^{(\mathrm{op})}]$ is calculated by the eigenmode solver. The imaginary part $\mathrm{Im}[E_z] = \mathrm{Im}[E_z^{(adj)}]$ is a pure adjacent mode contribution.

Table 1: RF Cavity Parameters

Frequency f_0	5.712 GHz
Mode separation Δf	10.0 MHz
Unloaded Q_0	11700
Coupling β	1.98
Loaded filling time τ_L	219 ns
Half-cell length L_{half} [(1)]	$0.61 \cdot \frac{\lambda_0}{2} = 16.008$ mm
Full-cells length L_{full} [(1)]	$0.97 \cdot \frac{\lambda_0}{2} = 25.558$ mm
Iris aperture i	10.000 mm
Iris topology	elliptic

[(1)] $\lambda_0 = c/f = 52.485$ mm.

additional ~ 10 MHz in mode separation while keeping the maximum surface electric field below the maximum electric field on-axis.

MAGNET DESIGN

With the presented RF coaxial coupling, the only mechanical constraints for the placement of the solenoid and bucking coil are the position of the input wave guide behind the cathode (longitudinal direction) and the outer diameter of the coupler (transverse direction).

This allows a mechanical simplification of the bucking coil and solenoid which can be combined into a single magnet as in the Poisson simulation of Fig. 4 (top). The two coils are driven with opposed current polarity in order to obtain zero field at the cathode which is required to avoid an additional emittance contribution [9].

The presented magnet fits with the gun RF design of Fig. 1 and the achievable maximum field on-axis $\max_z B_z \geq 0.4$ T is far above the required field for optimal beam dynamics

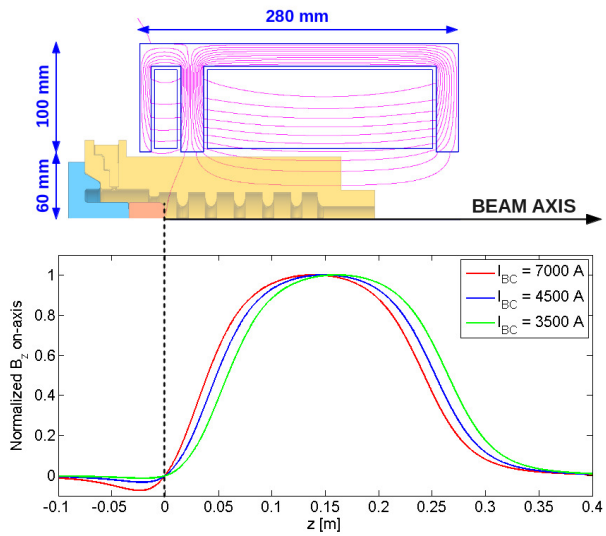

Figure 4: Magnetic field generated by the solenoid. 2D layout of the solenoid and field lines (top), and the corresponding longitudinal magnetic field B_z on-axis for different currents in the bucking coil (bottom).

ISBN: 978-3-95450-132-8 doi:10.18429/JACoW-IPAC2014-MOPRI043

(see Tab. 2). Adjusting the bucking coil current, the slope $dB_z/dz \approx -2/r \cdot B_r$ at the cathode can be tuned to obtain an optimal initial transverse focusing of the beam.

BEAM DYNAMICS

The presented 1D field profiles of the gun (Fig. 3) and solenoid (Fig. 4) have been used to optimize the beam dynamics of the SwissFEL injector with Astra and an in-house developed Matlab interface linked to the NL-OPT optimization library . Usually, four parameters are optimized: transverse laser spot size, gun phase, solenoid field strength and position of the first traveling-wave structure.

The conservative intrinsic emittance value of $\varepsilon_{intrinsic}/\sigma_{transv.} = 0.91$ μm/mm [10] was assumed in the simulations in order to allow an easier comparison with other designs. The achieved beam quality with the 5.6-cells C-band gun (see Tab. 2) is almost identical to that with a 3.6-cell C-band gun [6]: compared to the PSI Gun 1, the transverse brightness is doubled thanks to an increase in peak current while preserving the low mean slice emittance. The higher gun output energy due to the two additional cells and the relatively long solenoid shift the optimal position of the first traveling wave structure at 2.127 m from the cathode. This would provide more space for a complete beam diagnostic out of the gun, including a low energy spectrometer.

The effect on the beam dynamics of the adjacent mode in steady state was studied. After a reoptimization of laser spot size, gun phase and solenoid field strength, the typical tuning parameters during machine operation, no impact on the beam quality could be observed.

Table 2: Comparison of SwissFEL injector layout parameters and simulated beam quality at a beam energy > 100 MeV for the the new proposed design (C-band and the SwissFEL baseline design (S-band).

SwissFEL injector	**C-band gun**	**PSI Gun 1**
Laser pulse FWHM (1)	5.0 ps	9.9 ps
Laser transv. sigma(1)	0.174 mm	0.200 mm
Gun frequency	5.712 GHz	2.998 GHz
Gun design gradient	135 MV/m	100 MV/m
Gun phase (2)	−9.3 deg	−2.6 deg
Solenoid max. field	0.3549 T	0.2080 T
Solenoid max. field pos.	0.139 m	0.300 m
1. TW struct. pos.	2.274 m	3.3 m
1. TW struct. avg. grad.	18.2 MV/m	13.8 MV/m
Gun output energy	9.5 MeV	6.6 MeV
Peak current	37.4 A	20.0 A
Projected transv. emit.	0.26 μm	0.25 μm
Mean slice emit. (3)	0.21 μm	0.21 μm
Mean mismatch (3,4)	1.05	1.03
Transv. brightness (5)	6.87E13 A/m^2	3.6E13 A/m^2

(1) Flat-top transverse and temporal distribution of the laser pulse assumed.
(2) With respect to maximum energy gain.
(3) Mean over 20 slices, neglecting the 3 most external at the head and tail of the bunch.
(4) Definition used: $\zeta_s \equiv 1/2 \cdot (\beta_0\gamma_s - 2\alpha_0\alpha_s + \gamma_0\beta_s)$, where α, β, γ are the Twiss parameters for the whole bunch (index 0) and the single slice (index s).
(5) Definition used: $B_\perp \equiv 1/4\pi \cdot I_{peak}/\varepsilon^2_{slice}$.

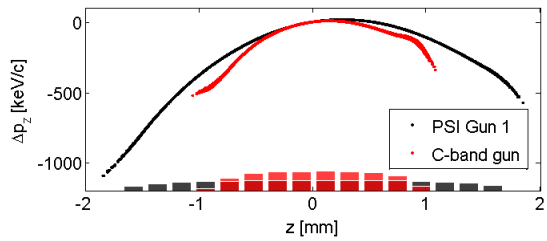

Figure 5: Longitudinal phase space after the second TW structure of the layouts compared in Tab. 2. The histograms represent the charge density distribution of the 200 pC bunch.

CONCLUSION

The feasibility of a C-band standing-wave photo-cathode gun as electron source for the SwissFEL injector was demonstrated by presenting an RF and magnet design which double the transverse beam brightness compared to the current baseline design.

In particular, an innovative coaxial coupling from the cathode side was presented and its several advantages were described. The effect of the adjacent mode in the transient regime is still under study, with the possibility to increase the mode separation up to ~ 20 MHz by increasing the iris aperture.

A careful thermal and RF tolerance analysis together with a mechanical design is still required.

ACKNOWLEDGMENT

The authors gratefully acknowledge Kabelwerke Brugg AG Holding, Fachhochschule Nordwestschweiz and Paul Scherrer Institut for the financial support to this project.

REFERENCES

[1] R. Bossart et al., “Design of an RF gun for heavy beam loading”, EPAC96 Proceedings, Barcelona, 1996.
[2] E. Prat et al., TUOCNO06, FEL13 Proc., New York, 2013.
[3] R. Ganter et al., SwissFEL CDR, PSI Report 10-04, 2012.
[4] J.-Y. Raguin et al., TUPLB01, LINAC12 Proc., Telaviv, 2012.
[5] S. Bettoni et al., TUPSO07, FEL13 Proc., New York, 2013.
[6] M. Schaer et al., MOPFI062, IPAC13 Proc., Shanghai, 2013.
[7] F. Wang, SLAC-PUB-13458, 2008.
[8] K. Floetmann, NIM A, 393, 93, 1997.
[9] M. Reiser, “Theory and design of charged particle beams”, WILEY-VCH, Weinheim, 2008.
[10] Y. Ding et al., Phys. Rev. Lett., 102, 254801, 2009.